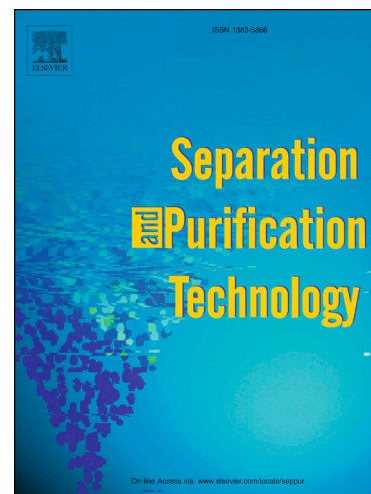


Accepted Manuscript

Tubular ultrafiltration ceramic membrane based on titania nanoparticles immobilized on macroporous clay-alumina support: Elaboration, characterization and application to dye removal

Abdallah Oun, Nouha Tahri, Samia Mahouche-Chergui, Benjamin Carbonnier, Swachchha Majumdar, Sandeep Sarkar, Ganesh C. Sahoo, Raja Ben Amar

PII: S1383-5866(17)31526-5
DOI: <http://dx.doi.org/10.1016/j.seppur.2017.07.005>
Reference: SEPPUR 13862



To appear in: *Separation and Purification Technology*

Received Date: 15 May 2017
Revised Date: 1 July 2017
Accepted Date: 2 July 2017

Please cite this article as: A. Oun, N. Tahri, S. Mahouche-Chergui, B. Carbonnier, S. Majumdar, S. Sarkar, G.C. Sahoo, R. Ben Amar, Tubular ultrafiltration ceramic membrane based on titania nanoparticles immobilized on macroporous clay-alumina support: Elaboration, characterization and application to dye removal, *Separation and Purification Technology* (2017), doi: <http://dx.doi.org/10.1016/j.seppur.2017.07.005>

This is a PDF file of an unedited manuscript that has been accepted for publication. As a service to our customers we are providing this early version of the manuscript. The manuscript will undergo copyediting, typesetting, and review of the resulting proof before it is published in its final form. Please note that during the production process errors may be discovered which could affect the content, and all legal disclaimers that apply to the journal pertain.

**Tubular ultrafiltration ceramic membrane based on titania nanoparticles
immobilized on macroporous clay-alumina support: Elaboration,
characterization and application to dye removal**

**Abdallah Oun ^{a,b,c}, Nouha Tahri ^a, Samia Mahouche-Chergui ^{b*}, Benjamin Carbonnier ^{b*},
Swachchha Majumdar ^c, Sandeep Sarkar ^c, Ganesh C. Sahoo ^c, and Raja Ben Amar ^{a*}**

^a *Laboratoire des Sciences de Matériaux et Environnement, Université de Sfax, Faculté des Sciences
de Sfax, BP 1171,3000, Sfax-Tunisia*

^b *Université Paris-Est, ICMPE (UMR7182), CNRS, UPEC, Thiais, 94320, France*

^c *CSIR-Central Glass and Ceramic Research Institute (CGCRI), 196, Raja S C Mullick Road, Kolkata
700032, India*

***Corresponding authors :**

*Raja BEN AMAR, Faculté des Sciences de Sfax, Laboratoire Sciences des Matériaux et
Environnement, Route de Soukra Km 4 BP 1171, Sfax, Tunisie. Tel: (+216) 74 276 400 /
(+216) 74 276 763; Fax: (+216) 74 274 437;
e-mail address: raja.rekik@fss.rnu.tn

*Samia Mahouche-Chergui, Maître de Conférences - Université Paris 12, Equipe "Systèmes
Polymères Complexes" (SPC) Bâtiment H, Rez-de-Chaussée, bureau 12
e-mail address: mahouche.samia@gmail.com

* Benjamin Carbonnier, Professeur - Université Paris-Est, Equipe "Systèmes Polymères
Complexes" (SPC), Bâtiment C, 1er étage, bureau 105, 2-8, rue H. Dunant F-94320 Thiais
e-mail address: carbonnier@icmpe.cnrs.fr

Abstract

The development of new membranes with improved separation properties, high mechanical and thermal stability using inexpensive and naturally abundant materials is of utmost importance for sustainable development and environmental applications. Ceramic materials due to their high chemical, mechanical and thermal stability in combination to their facile surface functionalization have inspired material scientists to design innovative low-cost ceramic-based membrane supports.

This study focuses on the preparation and characterization of novel asymmetric ultrafiltration ceramic membrane coated with single separation layer made of TiO_2 nanoparticles, and its application to removal of alizarin dye from aqueous solutions. The membrane was prepared by a simple and one-step deposition of micrometer-thick titania layer on the internal surface of the tubular-shape porous clay-alumina membrane support from an aqueous colloidal suspension of titanium oxide (TiO_2) nanoparticles with size of 10 nm. The colloidal suspension was prepared in the presence of 0.2 wt.% of Dolapix, and 30 g of an aqueous solution of polyvinyl alcohol at 12 wt.% and 66 mL of H_2O . Microfiltration tubular supports of 10 mm/7 mm (outer/inner diameter) were prepared through an extrusion method followed by a sintering process using China Clay Rajmahal grade and alumina, as mineral precursors. The composition of 25% of clay and 75% of alumina was selected in this work as it showed a lower sintering temperature ($T_f=1350^\circ\text{C}$) which could ensure low cost elaboration process, an average water flux of $850 \text{ L h}^{-1} \text{ m}^{-2} \text{ bar}^{-1}$ as well as enhanced mechanical performance ($\approx 37 \text{ MPa}$) and large porosity (48%) with an average pore diameter of $0.75 \text{ }\mu\text{m}$. SEM characterization showed that at the sintering temperature of 800°C , the TiO_2 nanoparticles coated densely and homogeneously the ceramic support forming a thin layer of about $4.2 \text{ }\mu\text{m}$ in thickness and leading to a clear reduction of the mean pore size (50 nm approximatively)

while providing a water permeability of $117 \text{ L.h}^{-1}.\text{m}^{-2}.\text{bar}^{-1}$. The so-designed ultrafiltration (UF) tubular ceramic membrane has proved efficient for alizarin red dye removal with a retention rate of 99% and a permeate flux of $70 \text{ L.h}^{-1}.\text{m}^{-2}$ at pH 9 and a transmembrane pressure of 5 bar.

KEYWORDS: ceramic membrane, TiO_2 separation layer, clay/alumina, ultrafiltration, tubular support, dye removal.

1. Introduction

Membrane separation technology has become increasingly appealing to address various scientific and technological issues associated to pollutions treatment. The wide variety of ceramic membranes meant for water treatment makes this technology very promising for both purification of drinking water and treatment of industrial wastewater containing emerging organic and inorganic pollutants. The success of ceramic membranes can be rationalized by their intrinsic properties, notably in terms of thermal and chemical stability and high mechanical strength [1-4]. It is well known that beside the chemical nature of membrane, its topology as well as its elaboration process influence strongly the membrane durability and resistance to harsh application conditions such as acidic and alkali media. Commercialized ceramic membranes are mainly manufactured from metal oxides such as alumina, silica, zirconia and titania [2-5]. Since the pioneering research in ceramic membranes technology, α -alumina has been mostly used as raw materials in varied fabrication processes [6].

Undoubtedly, the synergy between ceramic materials' precursors and advanced manufacture processes has led to considerable progresses providing new generations of high-performance

inorganic membranes combining well-defined morphological properties (such as porosity), physicochemical stability (pH), mechanical strength and high flow resistance (pressure), separation efficiency and selectivity [1,3,4,6,7]. These new generations of low cost ceramic membranes based on raw materials such as clay, starch, chamotte, apatite, and sand have been widely developed and studied on laboratory scale units working both in the microfiltration (MF) and ultrafiltration (UF) domains [8-18]. The UF process allows the removal of high molecular weight substances such as dyes [16,19] and can be easily integrated to biological wastewater treatment [19,20]. Among the plethora of inorganic precursors, kaolin clay has been intensively considered as pore forming agent raw material for the cost-effective design of stable inorganic membranes exhibiting a broad range of filtration processes [12-15].

In this context, this study is intended to elaborate tubular-shape porous membranes using extrusion method followed by sintering process using a mixture of natural kaolin clay and alumina powders as ceramic materials. The so-designed tubular ceramic tube served as solid support for the preparation of defect-free UF layer *via* slip-casting, using TiO₂ nanoparticles suspension. The rationale for using titania nanoparticles arises from their unique characteristics among which one may cite anti-fouling character, chemical stability [1,21,22], suitability for separation and antimicrobial efficiency [23], together with high photocatalytic activity [24-30]. It is assumed that incorporation of titania-based active layer into porous ceramic membranes may lead to improved separation performances in the different fields of membrane separation processes including microfiltration (MF), ultrafiltration (UF) and nanofiltration (NF) [22,24-26,31,32]. With the final aim to meet the legal requirements for the discharge of wastewater, the ceramic-titania-based UF single channel ceramic membrane was used for the removal of hazardous alizarin red, a popular indocile dye widely found in textile wastewater [33-35], from alizarin red-spiked aqueous solutions. As such, this paper assesses both the synthesis and characterization aspects of the hybrid membrane and discusses its

separation efficiency notably in terms of permeate flux and dye retention. Finally, the impact of operating parameters, namely transmembrane pressure (TMP), pH and dye initial concentration on the permeate flux and dye rejection rate is determined.

2. Experimental

2.1. Materials

The raw starting materials used for preparing the tubular porous membrane support are clay and alumina. The kaolin clay powder of Rajmahal grade, was first grinded with a ceramic mortar and then sieved to provide a granulometry of about 100 μm . α -Alumina powder (99 %) with a mean particle size of 7 μm was a kind gift from Hindalco company, India. Cellulose ether (methocel), polyvinyl alcohol (PVA, MW-13000-23000 $\text{g}\cdot\text{mol}^{-1}$) and anionic polyelectronic Dolapix (CE64) used as organic binder, plastisizer and dispersant agent, respectively, were purchased from Dow Chemical company. Titanium dioxide nanoparticles (TiO_2 , 98 %) with a mean particle size of 10 nm were purchased from Advanced Technology Materials, India. Alizarin red dye was used as a model textile dye to prepare spiked aqueous solutions and was purchased from Sigma-Aldrich.

2.2. Characterization and instruments

The mechanical strength of the sintered ceramic supports was measured by a three-point bending flexural test using an UTM Instron 5500 R (Software: Blue Hill, Universal Testing Machine of 10 tonnes capacity) to evaluate the effect of the clay-alumina composition and Methocel amount on the mechanical properties of the resulting membranes. The measurements were performed on sintered rectangular bars of 10 mm breadth, 5 mm height and 50 mm length using a span of 40 mm and a crosshead speed of 1.0 mm/min. Thermogravimetric (TGA) and differential (DTA) thermal analyses of the clay-alumina pastes

were performed using a Netzsch STA 449C apparatus (Germany) in a temperature range between 0 and 1500°C at a heating rate of 10°C/min under air atmosphere in order to determine the temperature-time schedule to be used for preparing the ceramic supports. Pore size of the tubular support was evaluated by means of mercury intrusion porosimetry (Micromeritics AutoPore IV 9500). Field Emission Scanning Electron Microscopy (FESEM) coupled with Energy Dispersive X-Ray (EDX) analysis was used to investigate the microstructure and analyze the surface morphology of both native clay-alumina support and corresponding UF membrane obtained after coating with a TiO₂ layer. The thickness of the TiO₂ layer was also determined from SEM images. To determine the transfer properties of native and TiO₂ coated supports, pure water flux and filtration tests were conducted using a home-made setup as schematically depicted in Fig. 1.

2.3. Preparation of tubular clay-alumina supports

Ceramic precursor pastes were prepared through blending different amounts of dry kaolinite clay, alumina and Methocel powders as presented in Table 1 [36].

Table 1: Composition of the ceramic supports and mixing conditions.

Sample name	Composition dry mineral basis (wt.%)		Organic binder (g)	Liquid Phase (g)	Dry Mixing time (min)	Wet Mixing time (min)
	Kaolin	Alumina	Methocel	Water		
C25A75M4	25	75	4	31	15	30
C25A75M6	25	75	6	30	15	30
C25A75M8	25	75	8	30	15	45
C25A75M10	25	75	10	28	15	45
C50A50M4	50	50	4	26	15	30
C50A50M6	50	50	6	30	15	30
C50A50M8	50	50	8	28	15	45
C50A50M10	50	50	10	30	15	45

Manufacturing of porous tubular ceramic supports was achieved *via* an extrusion process using a single screw type extruder (Brabender, Germany) (Fig. 1) [37]. After drying at room temperature, and sintering under a multi-step thermal treatment program for which the final temperature was set at $T_f = 1350^\circ\text{C}$ as shown in Fig. 1b, several tubular macroporous membrane supports with an ID = 7 mm and an OD = 10 mm were obtained (Fig. 1c). Support with 25% clay and 75% alumina and 6g of methocel, referred to as C25A75M6 hereafter, has been selected for the continuation of this work due to the formation of the high aspect mullite phase even at low temperature (1150°C) which ensure high mechanical resistance and better thermal and chemical stability [11].

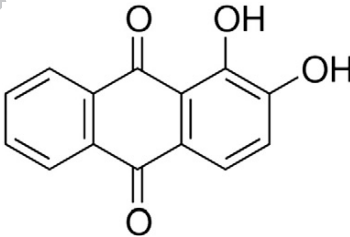
2.4. Design of TiO_2 -based tubular ceramic UF membrane

The active titania UF separation layer was prepared through slip casting process involving the deposition of the casting slurry on the support for an optimal contact time of 10 min. The slurry was prepared by dispersing, under magnetic stirring, 4g of titania powder in an aqueous solution containing well dispersed PVA (12 wt.%) and a low amount of Dolapix CE64 dispersant (0.2 wt.%). The latter improved the stability of the dispersion while the former acted as a binder and enhanced the viscosity of the solution to ensure homogenous casting of the titania nanoparticles on the inner surface of the tubular support membrane. The deposition of TiO_2 layer was ensured by mean of capillary suction inside the tubular support. Afterwards, the coated support was dried at ambient temperature for 24 h, followed by a calcination step at 800°C for 3h. It is important to note that in order to obtain cracks-free membrane, very low heating rate ($3^\circ\text{C}/\text{min}$) was used.

2.5. Cross flow ultrafiltration (UF)

The so-designed TiO₂ coated tubular porous ceramic membrane was applied to the decolorization of alizarin dye-containing solution by ultrafiltration. Major characteristics and chemical formula of alizarin dye are summarized in Table 2.

Table 2. Alizarin red dye characteristics.

Characteristic	Alizarin Red
Molecular formula	C ₁₄ H ₈ O ₄
Chemical name	1,2-Dihydroxy-9,10-anthraquinone
Molecular weight	240.21 g.mol ⁻¹
λ_{\max} (pH = 9)	260, 327 and 521 nm
pka	6.77
Class	Anthraquinone
Chemical structure	

Cross-filtration membrane tests were conducted using a home-made lab-scale unit. The filtration system is equipped with an adjustable outflow pump, a feed tank of 10 L capacity, and a stainless steel (316L) module hosting a single channel membrane (length of 300 mm, outer diameter of 10 mm and inner diameter of 7 mm). The effective membrane area was 65.94 cm² and the TMP was varied in the range between 1 and 8 bar. The permeate flux value through the membrane was measured as a function of time at different transmembrane pressures. Prior to permeability measurements, the membrane was conditioned by immersion in pure deionized water for at least 24 hours. Dye solutions were prepared by dissolving alizarin red in deionized water and the pH was adjusted to 9 by adding NaOH solution (1M).

All filtration tests were performed in triplicate and results are presented hereafter for the third filtration cycle.

3. Results and discussion

3.1. Design and characterization of macroporous tubular ceramic membranes

Morphological properties, chemical and mechanical stability are some of the key features to be finely controlled to design membrane materials with outstanding properties. To this aim, various ceramic-like precursor pastes were prepared based on different compositions of dry powders as summarized in table 1. Alumina versus kaolin ratio as well as amount of both aqueous phase and organic binder, namely methocel, was primarily investigated together with the wet mixing time (varied between 30 and 45 min) while the dry mixing time was kept constant at 15 min. Porous tubular ceramic supports were manufactured through an extrusion process using a single screw-type extruder and a thermal treatment involving two temperature steps (noted dwell in Fig. 1b) at 350 and 1350°C. Temperature rates of 3°C/min and 5°C/min were applied for heating up the samples from RT and 350°C, respectively.

3.1.1. Mechanical strength

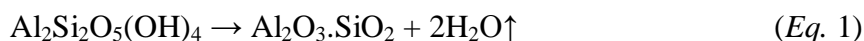
To control the resistance of the tubular support sintered at a temperature of 1350°C, mechanical resistance tests were performed on bar samples using the three-point bending flexural test. Effect of both the mass content of methocel and clay-alumina composition in the plastic paste membrane precursor on the mechanical properties of the membrane supports was investigated. It was observed for clay/alumina 50/50 tubular supports that the mechanical strength was improved from 32 to 40 MPa when the methocel binder content was increased from 4 to 6 g (Fig. 2a). Incorporation of more than 6 g of binder to the ceramic mixture was detrimental to mechanical strength of the resulting clay-alumina supports. This may be due to

a considerable increase in the porosity of the support. This finding suggests that 6 g of binder are optimal for ensuring good adhesion and uniformity of the ceramic structure associated with optimal rheological properties.

Clearly, an increase in the flexural strength of the ceramic tubular supports was observed for the initial paste mixture containing 25 wt.% of clay while the binder amount was kept constant and equal to 6 g (Fig. 2b). The increase in mechanical resistance as observed from about 12 MPa for pure alumina, to about 57 MPa for the composition 25wt.% clay and 75wt.% alumina may be explained by the formation of the mullite and cristobalite crystalline structures previously identified by TGA-DTA for sintered supports.

3.1.2. Thermal analysis

Both DTA and TGA thermograms were exploited to evaluate the sintering-mediated reaction between kaolin and alumina (fig. 3). The TGA curve for C25A75M6 support, selected in this work as support for the preparation of UF membrane, indicates weight loss of about 3 wt.% at low temperature (<100 °C). That is attributed to the evaporation of the intercalated or adsorbed water in the powder samples. The small weight loss of 4 wt.% seen in the TGA curve between 200 and 400°C can be attributed to the removal of structural water from the ceramic materials. This is confirmed by the corresponding DTA peak at about 330°C. The temperature range between 450°C and 550°C is associated to the second endothermic reaction. Regarding the TGA thermogram, such thermodynamic change corresponds to a sample mass loss of about 12 wt.%. This process arises from the burning out of the organic additives from the paste and the dehydration (structured water) of kaolin according to the reaction given in equation 1.



Accordingly, the structural hydroxyls are eliminated leading to the transformation of kaolin to a new metakaolin amorphous phase. [38-40]

In the high temperature regime, structural reorganization processes of the ceramic materials occur as suggested by the presence of a succession of exothermic phenomena located between 950°C and 1300°C. The complex nature of these reorganization phenomena is still the subject of many studies [38,41-43]. Identification of the involved mechanisms and determination of the chemical composition of the eventually resulting crystalline phases are often difficult and still uncertain, especially because the thermogravimetry curve does not show weight change of the ceramic material. Roy et al. [41] and Sahnoun et al. [44] showed that the exothermic peak located at about 1000°C is due to the structural reorganization of metastable metakaolin leading to the formation of gamma-alumina (γ -Al₂O₃) with spinel structure (Al-Si) according to the following chemical reaction:



The γ -alumina transitional phase could be at the origin of mullite formation (Eq. 3), which starts at about 1150°C to give firstly the primary, then secondary mullites followed by the cristobalite phase formation [42,45-47] according to:



3.1.3. Porosity and pore size distribution

The pore size distribution curves of the sintered C25A75M6 support is illustrated in Fig. 4. It can be observed a well-defined peak showing an average pores diameter ranging from 0.20 to 7 μm , and centered at 0.75 μm . This reveals a monomodal and uniform pore size distribution which evidences the success of the extrusion process and the absence of cracks throughout the support.

3.1.4. Morphology

Fig. 5 shows the FESEM images of the inner surface of the ceramic membrane C25A75M6 sintered at 1350°C. The support microstructure indicates a high densification and homogeneous surface. The absence of cracks and the uniformity of the surface of the support shown both by SEM and mercury intrusion porosimetry are considered as key features for enhanced retention of the titania nanoparticles, allowing the deposition of continuous and dense coating layer.

3.2. Characterization of TiO₂-coated C25A75M6 ultrafiltration membrane

3.2.1 Morphology

The titania thin layer as elaborated after calcination at 800°C for 3h was analyzed and imaged by FESEM. The microstructure observations of the surface and the cross-section are shown in Fig. 6. Fig. 6a shows that smooth and homogeneous inner surface was obtained with a mean pore diameter of about 50 nm. According to the cross-section image of the membrane, asymmetric structure was observed with TiO₂ nanoparticles tightly packed and well attached to the internal surface of the tubular support. This active filtration layer exhibits an approximate thickness of 4.2 μm (Fig. 6b).

3.2.2 Water permeability and permeate flux

In order to assess the effect of the deposited titania layer, comparison between water permeability of the pristine tubular support and the UF membrane has been accomplished using pure water. Before starting the measurements, membrane samples were immersed in deionized water for 24 h. As shown in fig. 7, the water permeate flux increases linearly with the applied transmembrane pressure (TMP). The permeability of the membrane is remarkably decreased from $850 \text{ L h}^{-1} \text{ m}^{-2} \text{ bar}^{-1}$ for the native support to $117 \text{ L h}^{-1} \text{ m}^{-2} \text{ bar}^{-1}$ for the TiO_2 coated membrane. The permeability value determined for the TiO_2 -coated membrane is typical for UF membrane. This result indicates that the TiO_2 layer is responsible for the permeability decrease that can be explained by the lower pore size of UF titania active layer deposited on the C25A75M6 support providing further evidence of its robust embedding in the membrane support.

In addition, the effect of the TMP on the permeate flux (J_f) has been evaluated at room temperature and at pH 9 for three initial dye concentrations (150, 200 and 300 ppm). Similar time-dependences of the permeate flux (J_f) were observed for TMP values ranging from 1 bar to 8 bar (Fig. 8). Indeed, the permeate flux decreases continuously during the first 20 min of treatment then becomes quasi-constant. The higher stabilized flux of $140 \text{ L h}^{-1} \text{ m}^{-2}$ is obtained at the higher applied TMP of 8 bar. The stabilized flux decreases with decrease in the TMP becoming equal to $70 \text{ L h}^{-1} \text{ m}^{-2} \text{ bar}^{-1}$ for a TMP of 1 bar. This initial behavior showing a decline of the permeate flux is typical of UF membrane process and can be explained by the membrane fouling due to the interaction between the spiked solution and the membrane surface [48].

3.3. Application of TiO₂-coated C25A75M6 ultrafiltration membrane to decolorization of alizarin dye aqueous solution

In this work, the TiO₂-coated C25A75M6 membrane has been applied to color removal from aqueous solutions using alizarin red (ALZ-Red) as a model of textile dye. Efficiency of the decolorization expressed by retention percentage has been studied as a function of the initial dye concentration (150 ppm, 200 ppm and 300 ppm), pH of the dye solutions (2 to 12) and the TMP (1 to 8 bar). The retention percentage, denominated R (%), was obtained using the following equation:

$$R (\%) = 100 (1 - C_p/C_0).$$

Where C_p (ppm) is the permeate dye concentration and C_0 (ppm) the initial dye concentration.

3.3.1. Effect of pH of the feed dye solution

Efficiency of ALZ-Red removal was assessed at pH values varying from 2 to 12 for a feed concentration of 150 ppm and a separation time of 100 min (**Fig. 9**). It is worthy to note that the results shown in figures 8, 9 and 10 were obtained after the third repeated test of filtration. Purification and regeneration of the membranes were performed between each filtration cycle using, first, distilled water for 15 min, sodium hydroxide solution (2wt. %) at 80 °C for 20 min, nitric acid solution (2 wt. %) at 60 °C for 20 min, and finally water rinsing until reaching neutral pH. No significant decrease in filtration efficiency was observed in these conditions. It is clearly seen that efficiency of the UF process of alizarin depends strongly on the pH of the feed solution. Indeed, in an alkaline medium, the elimination is much more efficient than in an acid one, and it is almost total ($R > 98\%$) at pH 9. In contrast, in acidic medium the disappearance of alizarin was about twice as low. The change is observed in a rather narrow pH range, between 6 and 8, in correspondence to both pK_a (6.77) value and isoelectric point (~ 6) of alizarin and titanium dioxide, respectively. Although comprehensive discussion of the

mechanism of dye removal requires further investigations, it may be assumed that efficiency of the UF process results from a delicate balance of filtration process and interaction between the membrane and the alizarin solution. Such interactions are pH-dependent and controlled by the zeta potential and charge state of the TiO_2 top layer and alizarin, respectively. At low pH (< 6) titania layer may be in a protonated form that is detrimental to the separation efficiency. According to these results, pH of 9 was considered as optimum pH for the alizarin dye elimination by TiO_2 membrane and it was retained for the following study. Moreover, wastewater from the textile processing industry is often characterized by high pH [49] and, in the case of ALZ-Red, solubility was improved in alkaline medium.

3.3.2. Effect of the concentration of the feed dye solution

This study was carried out in order to evaluate retention efficiency over time of the TiO_2 -coated C25A75M6 membrane towards ALZ-Red solutions with different dye concentrations. The Fig. 10 shows two different regimes. Initially (time < 20 min), the retention rate assumes a steep increase and the increase is steeper for low concentrations. Then, for longer time, the retention rate levels off and a plateau regime is reached faster for the lower concentration, after about 60 min for 150 ppm to be compared to more than 120 min for 300 ppm. Nearly total retention is achieved faster for lower dye concentration. Indeed, in the course of the filtration process, dye molecules may adsorb onto the membrane surface driving to the formation of a cake layer. This effect is more pronounced for high dye concentration. As previously reported, accumulation of dye molecules may lead to clogging of the pores of the membrane leading to a compaction of the cake layer accompanied with a polarization phenomenon [50]. These combined effects often resulting in a decline of the permeate flux.

3.3.3. Effect of transmembrane pressure

As it can be observed in fig. 11, the color retention, as evaluated at a concentration of 150 ppm, was strongly dependent on the applied TMP. Low TMP (1 and 3 bars) provided limited retention efficiency. The highest retention rate of about 99% was observed from a TMP of 5 bar. It is important to note that the treated water became visually very clear after treatment at 5 or 8 bars (inset in **Fig. 11**). The very high permeate quality confirms the performances of the asymmetric UF titania membrane towards colour removal from dye polluted water. The retention of dye observed is assumed to arise from a dual functionality of the titania layer, namely adsorption and filtration [51,52].

4. Conclusion

In this study, a novel ultrafiltration clay-alumina membrane coated with a titania layer was successfully elaborated via a combination of extrusion, sintering and slip casting methods. FESEM, EDX, TGA, DTA and mechanical tests were applied to investigate the effects of the content of clay, alumina and methocel binder on physical and mechanical properties of the supports. Optimal thermal stability and mechanical properties were obtained for the membrane prepared from a composition made of 25wt.% kaolin clay, 75wt.% alumina and 6% of methocel. The ultrafiltration layer, based on titanium oxide nano-powder deposited onto the surface of the clay-alumina membrane support (C25A75M6) has a thickness of 4.2 μm and a mean pore size of 50 nm. The as-designed UF membrane exhibited a water permeability of 117 $\text{L.m}^{-2} \text{h}^{-1} \text{bar}^{-1}$, indicating that the titania layer is responsible for the decrease in permeability which was calculated to be 850 $\text{L.m}^{-2} \text{h}^{-1} \text{bar}^{-1}$ for the clay-alumina support with pristine surface. Finally, the ultrafiltration membrane was applied to the decolorization of dye containing aqueous solutions. Under optimal operating conditions, i.e.,

transmembrane pressure of 5 bars, pH=9 and dye concentration of 150 ppm, the TiO₂-coated membrane exhibited significant retention efficiency towards alizarin red dye as color removal of 99% was achieved. Hence, the newly designed titania-based membrane may open new avenues for the treatment of raw textile wastewater.

ACKNOWLEDGMENTS

The authors would like to thank Mr Rémy PIRES BRAZUNA, Assistant Engineer, for his assistance in scanning microscopy analysis.

References

- [1] T.V. Gestel, C. Vandecasteele, A. Buekenhoudt, C. Dotremont, J. Luyten, R. Leysen, Alumina and titania multilayer membranes for nanofiltration: preparation, characterization and chemical stability, *J. Membr. Sci.* 207 (2002) 73–89.
- [2] T.V. Gestel, H. Kruidhof, D.H.A. Blank, H.J.M. Bouwmeester, ZrO₂ and TiO₂ membranes for nanofiltration and per vaporation Part1. Preparation and characterization of a corrosion-resistant ZrO₂ nanofiltration membrane with a MWCO<300, *J. Membr. Sci.* 284 (2006) 128–136.
- [3] R.F.S. Lenza, W.L. Vasconcelos, Synthesis and properties of microporous sol–gel silica membranes, *J. Non-Cryst. Solids.* 273 (2000) 164–169.
- [4] G.E. Romanos, Th.A. Steriotis, E.S. Kikkinides, N.K. Kanellopoulos, V. Kasseelouri, et al., Innovative methods for preparation and testing of Al₂O₃ supported silicalite-I membranes, *J. Eur. Ceram. Soc.* 21 (2001) 119–126.

- [5] S. Chowdhury, R. Schmuhl, K. Keizer, J. Ten Elshof, D. Blank, Pore size and surface chemistry effects on the transport of hydrophobic and hydrophilic solvents through mesoporous γ -alumina and silica MCM-48, *J. Membr. Sci.* 225 (2003) 177–186.
- [6] K.A. Defriend, M.R. Wiesner, A.R. Barron, Alumina and Aluminate ultrafiltration membranes, *Chem. Bio. Eng Reviews* 2. (2003) 54-70.
- [7] Q. Chang, Y. Wang, S. Cerneaux, J. Zhou, X. Zhang, X. Wang, Y. Dong, Preparation of microfiltration membrane supports using coarse alumina grains coated by nano TiO_2 as raw materials, *J. Eur. Ceram. Soc.* 34 (2014) 4355–4361.
- [8] M.-M. Lorente-Ayza, S. Mestre, V. Sanz, E. Sánchez, On the underestimated effect of the starch ash on the characteristics of low cost ceramic membranes, *Ceramics International*. 42 (2016) 18944–18954.
- [9] M.-M. Lorente-Ayza, E. Sánchez, V. Sanz, S. Mestre, Influence of starch content on the properties of low-cost microfiltration ceramic membranes, *Ceramics International*. 41 (2015) 13064–13073.
- [10] J.-H. Ha, J. Lee, I.-H. Song, S.-H. Lee, The effects of diatomite addition on the pore characteristics of a pyrophyllite support layer, *Ceramics International*. 41 (2015) 9542-9548.
- [11] Z. Zhu, Z. Wei, W. Sun, J. Hou, B. He, Y. Dong, Cost-effective utilization of mineral-based raw materials for preparation of porous mullite ceramic membranes via in-situ reaction method, *Appl. Clay. Sci.* 120 (2016) 135–141.
- [12] B.K. Nandi, R. Uppaaluri, M.K. Purkait, Preparation and characterization of low cost ceramic membranes for microfiltration applications, *Appl. Clay. Sci.* 42 (2008) 102–110.
- [13] I. Hedfi, N. Hamdi, E. Srasra, M.A. Rodríguez, The preparation of micro-porous membrane from a Tunisian kaolin, *Appl. Clay. Sci.* 101 (2014) 574–578.

- [14] I. Hedfi, N. Hamdi, M.A. Rodriguez, E. Srasra, Development of a low cost micro-porous ceramic membrane from kaolin and Alumina, using the lignite as porogen agent, *Ceram. Int.* 42 (2016) 5089–5093.
- [15] M. Issaoui, L. Limousy, B. Lebeau, J. Bouaziz, M. Fourati, Design and characterization of flat membrane supports elaborated from kaolin and aluminum powders, *C. R. Chimie*, 19 (2016) 496-504.
- [16] M. Khemakhem, S. Khemakhem, S. Ayedi, R. Ben Amar, Study of ceramic ultrafiltration membrane support based on phosphate industry subproduct: application for the cuttlefish conditioning effluents treatment, *Ceram. Int.* 37 (2011) 3617-3625.
- [17] N. Saffaj, M. Persin, S.A. Younsi, A. Albizane, M. Cretin, A. Larbot, Elaboration and characterization of microfiltration and ultrafiltration membranes deposited on raw support prepared from natural Moroccan clay: Application to filtration of solution containing dyes and salts, *Appl. Clay. Sci.* 31 (2006) 110–119.
- [18] G. Sahoo, R. Halder, I. Jedidi, A. Oun, H. Nasri, P. Roychoudhury, S. Majumdar, S. Bandyopadhyay, R. Ben Amar, Preparation and characterization of microfiltration apatite membrane over low cost clay-alumina support for decolorization of dye solution, *Desalination and Water Treatment*. 57 (2016) 27700-27709.
- [19] E. Alventosa-deLara, S. Barredo-Damas, M.I. Alcaina-Miranda, M.I. Iborra-Clar, Ultrafiltration technology with a ceramic membrane for reactive dye removal: Optimization of membrane performance, *J. Hazard. Mater.* 209– 210 (2012) 492– 500.
- [20] B. Chamam, M. Heran, A. Grasmick, R. Ben Amar, Comparison of textile dye treatment by biosorption and membrane bioreactor, *Environ. Technol.* 28 (2007) 1-9.
- [21] R.R. Bhawe, *Inorganic Membranes Synthesis Characteristics and Applications*, Van Nostrand Reinhold, New York, 1991.

- [22] Z. Song, M. Fathizadeh, Y; Huang, K.H. Chu, Y. Yoon, L. Wang, W.L., Xu, M. Yu, TiO₂ nanofiltration membranes prepared by molecular layer deposition for water purification, *J. Membr. Sci.* 510 (2016) 72–78.
- [23] N. Saffaj, M. Persin, S.A. Younssi, A. Albizane, M. Bouhria, H. Loukili, H. Dach, A. Larbot, Removal of salts and dyes by low ZnAl₂O₄–TiO₂ ultrafiltration membrane deposited on support made from raw clay, *Sep. Purif. Technol.* 47 (2005) 36–42.
- [24] R. Goei, T.T. Lim, Asymmetric TiO₂ hybrid photocatalytic ceramic membrane with porosity gradient: Effect of structure directing agent on the resulting membranes architecture and performances, *Ceram. Inter.* 40 (2014) 6747–6757.
- [25] A. Alem, H. Sarpoolaky, M. Keshmiri, Titania ultrafiltration membrane: Preparation, characterization and photocatalytic activity, *J. Eur. Ceram. Soc.* 29 (2009) 629–635.
- [26] Y.H. Wang, X.Q. Liu, G.Y. Meng, Preparation of asymmetric pure titania ceramic membranes with dual functions, *Mater. Sci. Eng. A.* 445–446 (2007) 611–619.
- [27] S. Leong, A. Razmjou, K. Wang, K. Hapgood, X. Zhang, H. Wang, TiO₂ based photocatalytic membranes: A review, *J. Membr. Sci.* 472 (2014) 167–184.
- [28] R. Das, S. Sarkar, S. Chakraborty, H. Choi, C. Bhattacharjee, Remediation of Antiseptic Components in Wastewater by Photocatalysis Using TiO₂ Nanoparticles, *Ind. Eng. Chem. Res.* 53 (2014) 3012–3020.
- [29] S. Sarkar, K. Sondhi, R. Das, S. Chakraborty, H. Choi, C. Bhattacharjee, ‘a’, Development of a mathematical model to predict different parameters during pharmaceutical wastewater treatment using TiO₂ coated membrane, *Ecotoxi. Environ. Safety.* 121 (2015) 193–198.
- [30] S. Sarkar, S. Chakraborty, C. Bhattacharjee, ‘b’, Photocatalytic degradation of pharmaceutical wastes by alginate supported TiO₂ nanoparticles in packed bed photo reactor (PBPR), *Ecotoxi. Environ. Safety.* 121 (2015) 263–270.

- [31] P. Puhlfürß, A. Voigt, R. Weber, M. Morbé, Microporous TiO₂ membranes with a cut off <500 Da, *J. Membr. Sci.* 174 (2000) 123-133.
- [32] Y. Cai, Y. Wang, X. Chen, M. Qiu, Y. Fan, Modified colloidal sol–gel process for fabrication of titania nanofiltration membranes with organic additives, *J. Membr. Sci.* 476 (2015) 432–441.
- [33] T. Polubesova, M. Epstein, S. Yariv, I. Lapides, S. Nir, Adsorption of alizarinate–micelle complexes on Na-montmorillonite, *Appl. Clay. Sci.* 24 (2004) 177 – 183.
- [34] H. Sadegh, R. Shahryari-ghoshekandi, I. Tyagi, S. Agarwal, V.K. Gupta, Kinetic and thermodynamic studies for alizarin removal from liquid phase using poly-2-hydroxyethyl methacrylate (PHEMA), *J. Molec. Liq.* 207 (2015) 21–27.
- [35] M.L. De Souza, P. Corio, Effect of silver nanoparticles on TiO₂-mediated photodegradation of Alizarin Red S, *Appl. Catalysis B: Environ.* 136– 137 (2013) 325– 333.
- [36] S. Sarkar, S. Bandyopadhyay, A. Larbot, S. Cerneaux, New clay–alumina porous capillary supports for filtration application, *J. Membr. Sci.* 392– 393 (2012) 130– 136.
- [37] M. Ray, P. Bhattacharya, R. Das, K. Sondhi, S. Ghosh, S. Sarkar, Preparation and characterization of macroporous pure alumina capillary membrane using boehmite as binder for filtration application, *J. Porous Mater.* 22 (2015) 1043-1052.
- [38] F. Sahnoune, M. Chegaar, N. Saheb, P. Goeuriot, F. Valdivieso, ‘a’, Algerian kaolinite used for mullite formation, *Appl. Clay. Sci.* 38 (2008) 304 – 310.
- [39] A. Ghorbel, M. Fourati, J. Bouaziz, Microstructural evolution and phase transformation of different sintered Kaolins powder compacts, *Mater. Chem. Phys.* 112 (2008) 876– 885.
- [40] G.L. Lecomte, J.P. Bonnet, P. Blanchart, A study of the influence of muscovite on the thermal transformations of kaolinite from room temperature up to 1100°C, *J. Mater. Sci.* 42 (2007) 8745–8752.

- [41] R. Roy, D.M. Roy, E.E. Francis, New Data on Thermal Decomposition of Kaolinite and Halloysite, *J. Am. Ceram. Soc.* 38 (1955) 198-205.
- [42] O. Castelein, B. Soulestin, J.P. Bonnet, P. Blanchart, The influence of heating rate on the thermal behavior and mullite formation from a kaolin raw material, *Ceram. Int.* 27 (2001) 517–522.
- [43] W.E. Lee, G.P. Souza, C.J. McConville, T. Tarvornpanich, Y. Iqbal, Mullite formation in clays and clay-derived vitreous ceramics, *J. Eur. Ceram. Soc.* 28 (2008) 465–471.
- [44] F. Sahnoune, M. Chegaar, N. Saheb, P. Goeuriot, F. Valdivieso, ‘b’, Differential thermal analysis of mullite from Algerian kaolin, *Adv. Appl. Ceram.* 107 (2008) 9-13.
- [45] F. Bergaya, P. Dion, J.F. Alcover, C. Clinard, D. Tchoubar, TEM study of kaolinite thermal decomposition by controlled-rate thermal analysis, *J. Mater. Sci.* 31 (1996) 5069-5075.
- [46] Z. Chen, L. Zhang, Novel Method of adding seeds for preparation of mullite, *J. Mat. Proc. Tech.* 166 (2005) 183-187.
- [47] C.Y. Chen, W.H. Tuan, The processing of kaolin powder compact, *Ceram. Int.* 27 (2001) 795-800.
- [48] E. Ellouze, D. Ellouze, A. Jrad, R. Ben Amar, Treatment of synthetic textile wastewater by combined chemical coagulation/membrane processes, *Desalination and Water Treatment* 33 (2011) 118-124.
- [49] N. Tahri, G. Masmoudi, E. Ellouze, A. Jrad, P. Drogui, R. Ben Amar, Coupling microfiltration and nanofiltration processes for the treatment at source of dyeing-containing effluent, *Journal of Cleaner Production.* 33 (2012) 226-235.
- [50] B. Van der Bruggen, G. Cornelis, C. Vandecasteele, I. Devrees, Fouling of nanofiltration and ultrafiltration membranes applied for wastewater regeneration in the textile industry, *Desalination.* 175 (2005) 111–119.

[51] Z. Xiang, C. Di, W. Zhiwei, L. Yang, C. Rong, Nano-TiO₂ membrane adsorption reactor (MAR) for virus removal in drinking water, Ch. Eng. J. 230 (2013) 180–187.

[52] X. Zhang, Y. Wang, Y. You, H. Meng, J. Zhang, X. Xu, Preparation, performance and adsorption activity of TiO₂ nanoparticles entrapped PVDF hybrid membranes, Appl. Surf. Sci. 263 (2012) 660–665.

FIGURE CAPTIONS

Fig. 1. (a) Schematic representation of the home-made cross flow UF membrane set up. (b) Firing schedule applied for the preparation of the porous tubular ceramic supports. (c) Photograph of extruded porous tubular ceramic supports sintered at a temperature of 1350°C for 90 min.

Fig. 2. Effect of (a) methocel and (b) clay contents on the mechanical strength of the porous tubular ceramic supports sintered at a temperature of 1350°C for 90 min. In a) the clay/alumina ratio is 50/50 while in b) the methocel content was kept constant at 6g.

Fig. 3. TGA and DTA plots recorded for the porous tubular ceramic support C25A75M6 prepared from the composition clay/alumina/methocel 25/75/6 and sintered at a temperature of 1350°C for 90 min.

Fig. 4. Pore size distribution measured for the porous tubular ceramic support C25A75M6 prepared from the composition clay/alumina/methocel 25/75/6 and sintered at a temperature of 1350°C for 90 min.

Fig. 5. Field emission scanning electron microscopy images of a) top surface and b) cross section of the porous tubular ceramic support C25A75M6 prepared from the composition clay/alumina/methocel 25/75/6 and sintered at a temperature of 1350°C for 90 min.

Fig. 6. Field emission scanning electron microscopy images of a) top-surface and (b) cross-section of ceramic membrane support C25A75M6 prepared from the composition clay/alumina/methocel 25/75/6 and coated with a TiO_2 layer. The inset in part a) shows a magnified image of the TiO_2 -based membrane's surface.

Fig. 7. Variation of the water permeability as a function of the transmembrane pressure for the ceramic membrane support C25A75M6 (square) before and (circle) after coating with TiO_2 layer.

Fig. 8. Time-dependences of the flux of alizarin red solutions at different transmembrane pressures for the ceramic membrane support C25A75M6 coated with a TiO_2 layer. UF conditions: $[\text{ALZ}] = 150 \text{ ppm}$ and $\text{pH} = 9$.

Fig. 9. Variation of the retention rate (R , expressed in %) of Alizarin Red as a function of the pH of the dye solution as measured for the ceramic membrane support C25A75M6 coated with a TiO_2 layer. UF conditions: $[\text{ALZ}] = 150 \text{ ppm}$, $\text{TMP} = 5 \text{ bar}$ and $t=100 \text{ min}$.

Fig. 10. Time-dependences of the retention rate (R , expressed in %) for various initial concentrations of Alizarin Red as measured for the ceramic membrane support C25A75M6 coated with a TiO_2 layer. UF conditions: $\text{TMP} = 5 \text{ bar}$ and $\text{pH} = 9$.

Fig. 11. Variation of the retention rate of alizarin red dye from spiked water solution (150 ppm) as a function of the transmembrane pressure. The insets showing images of the feed dye solution (left) and the permeate solution (right) as obtained after ultrafiltration process during 100 min at 5 bar evidence the effectiveness of dye removal.

Fig. 1.

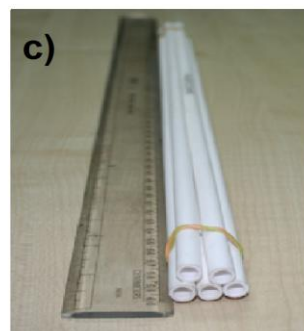
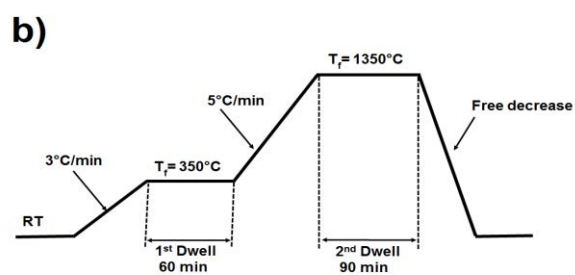
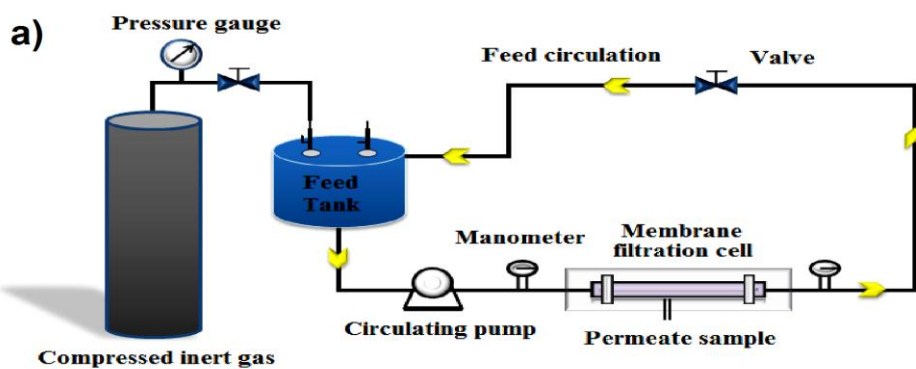


Fig. 2.

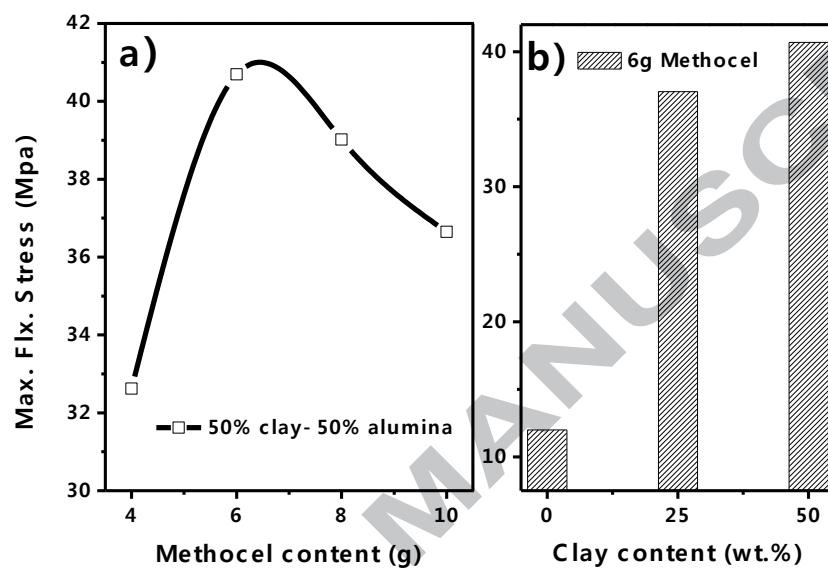


Fig. 3.

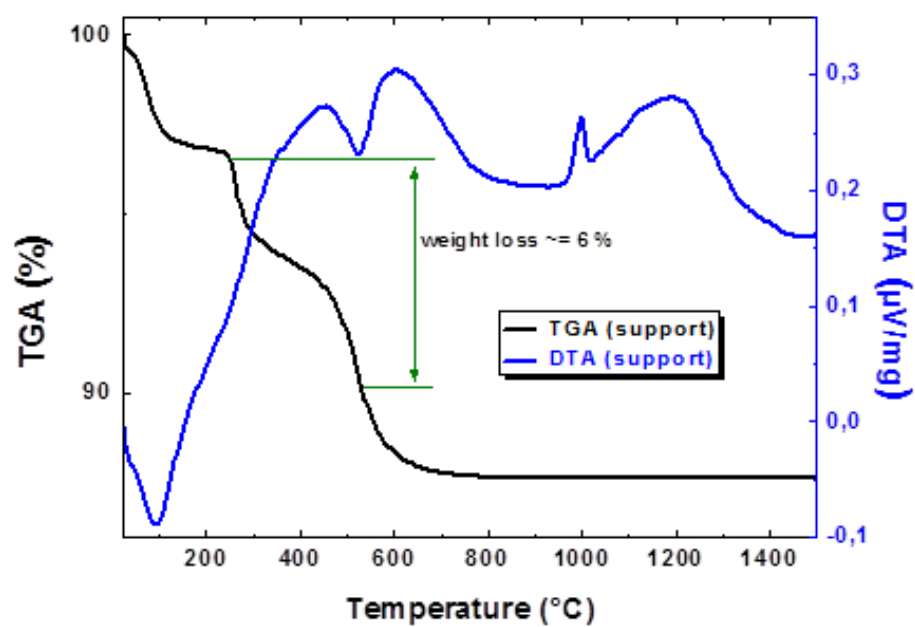


Fig. 4.

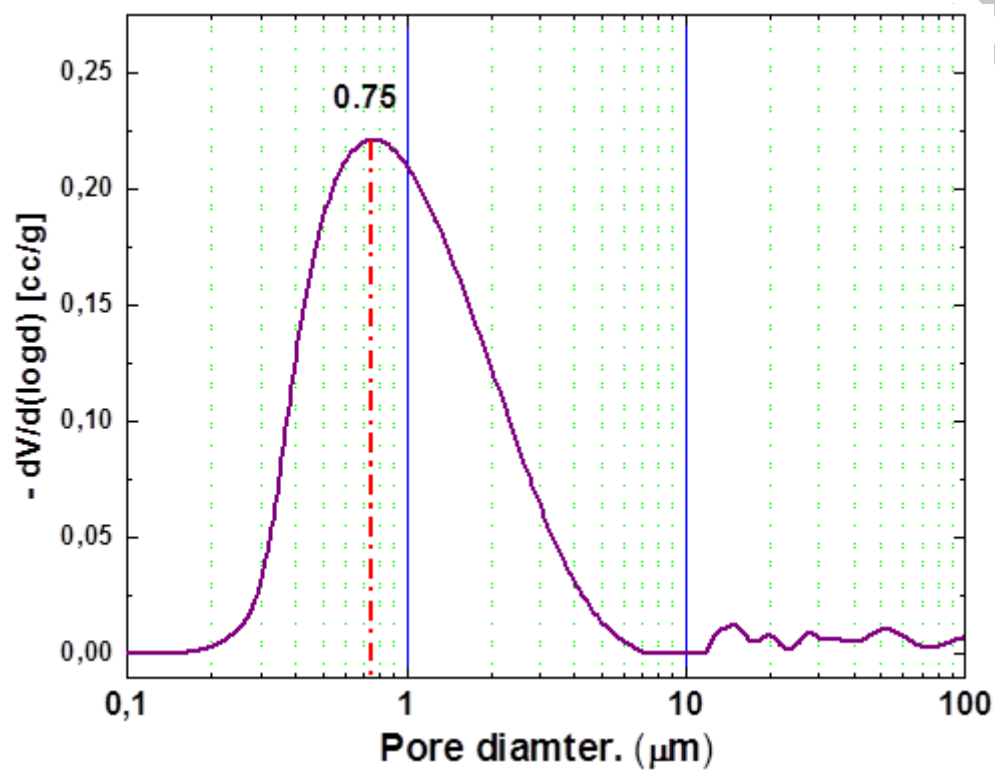


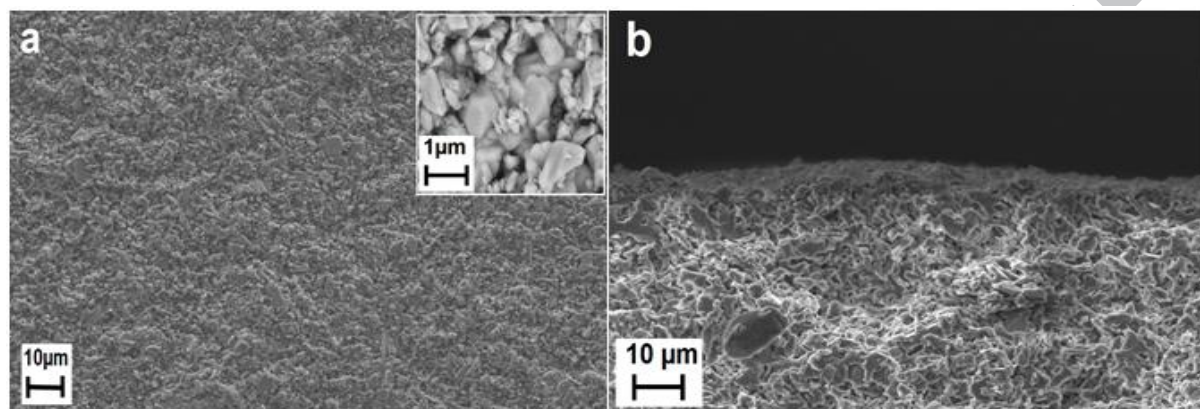
Fig. 5.

Fig. 6.

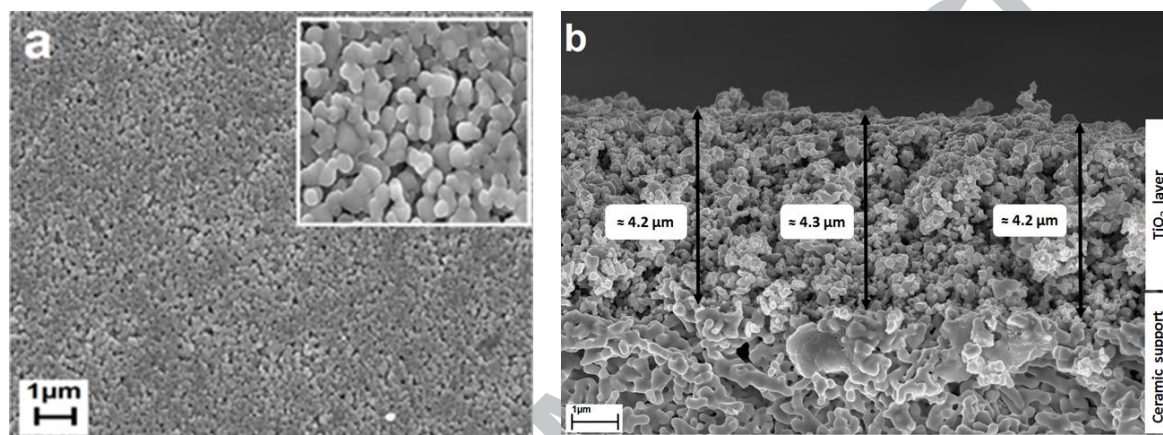


Fig. 7.

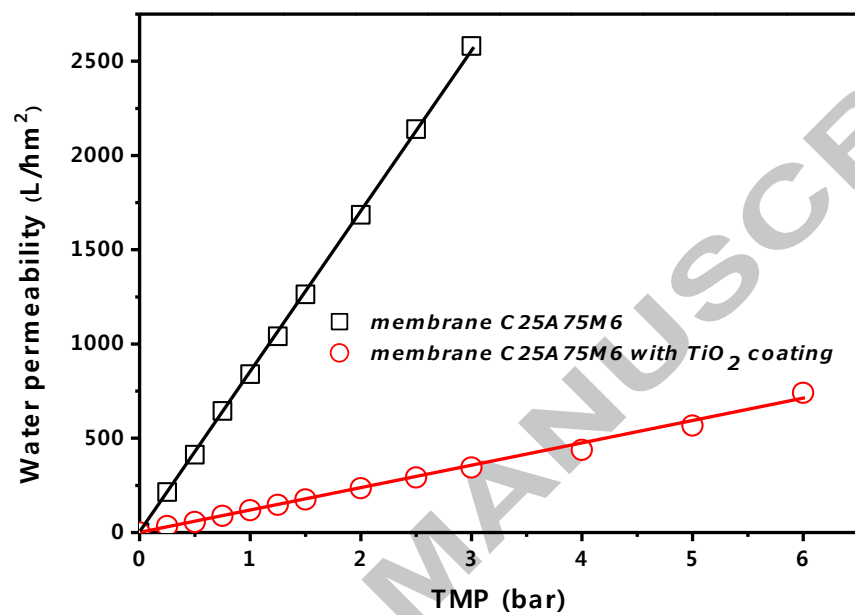


Fig. 8.

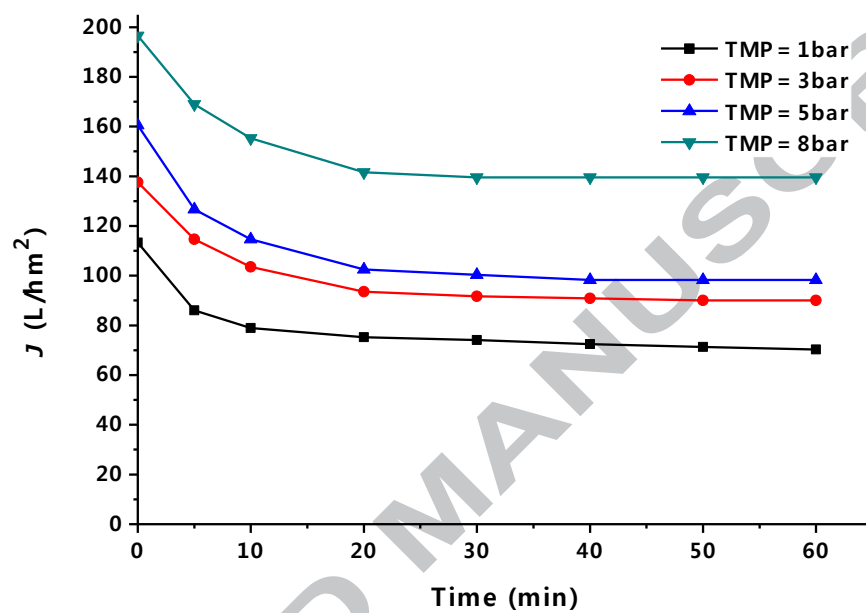


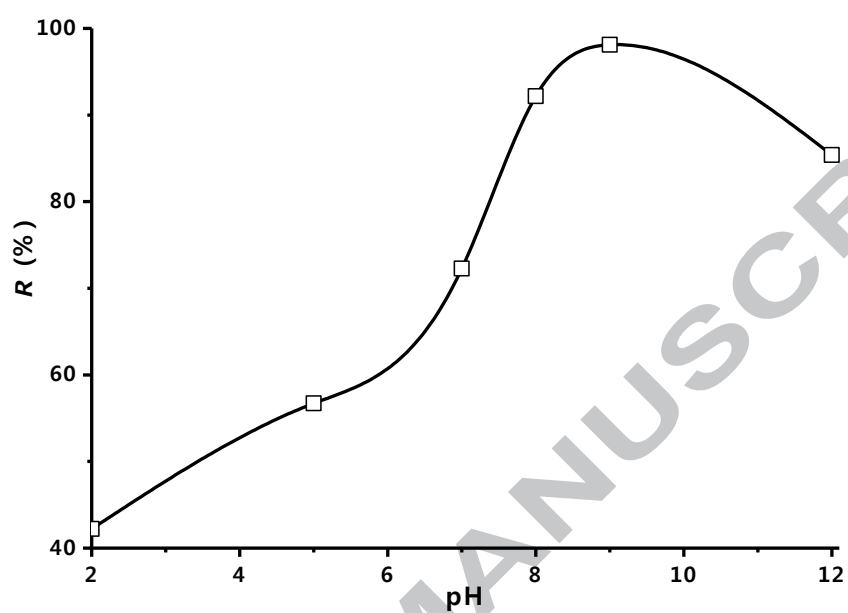
Fig. 9.

Fig. 10.

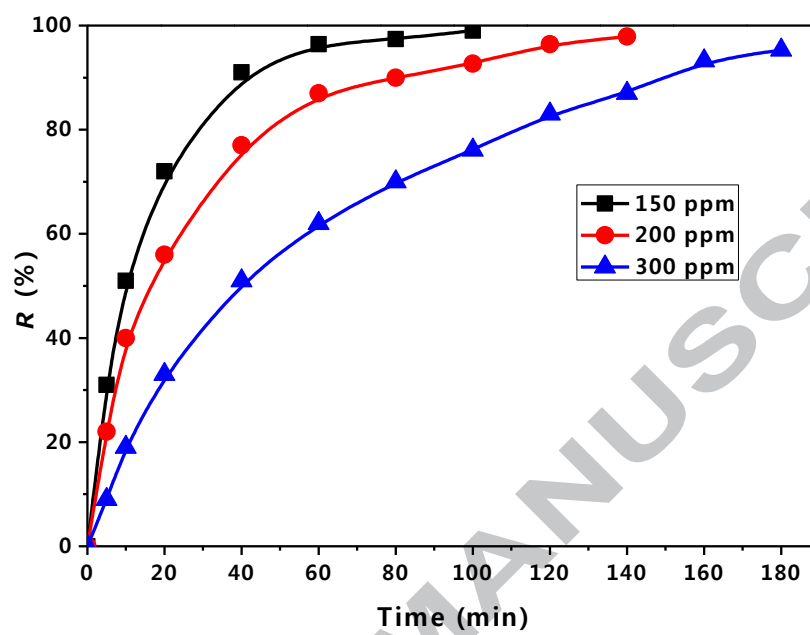
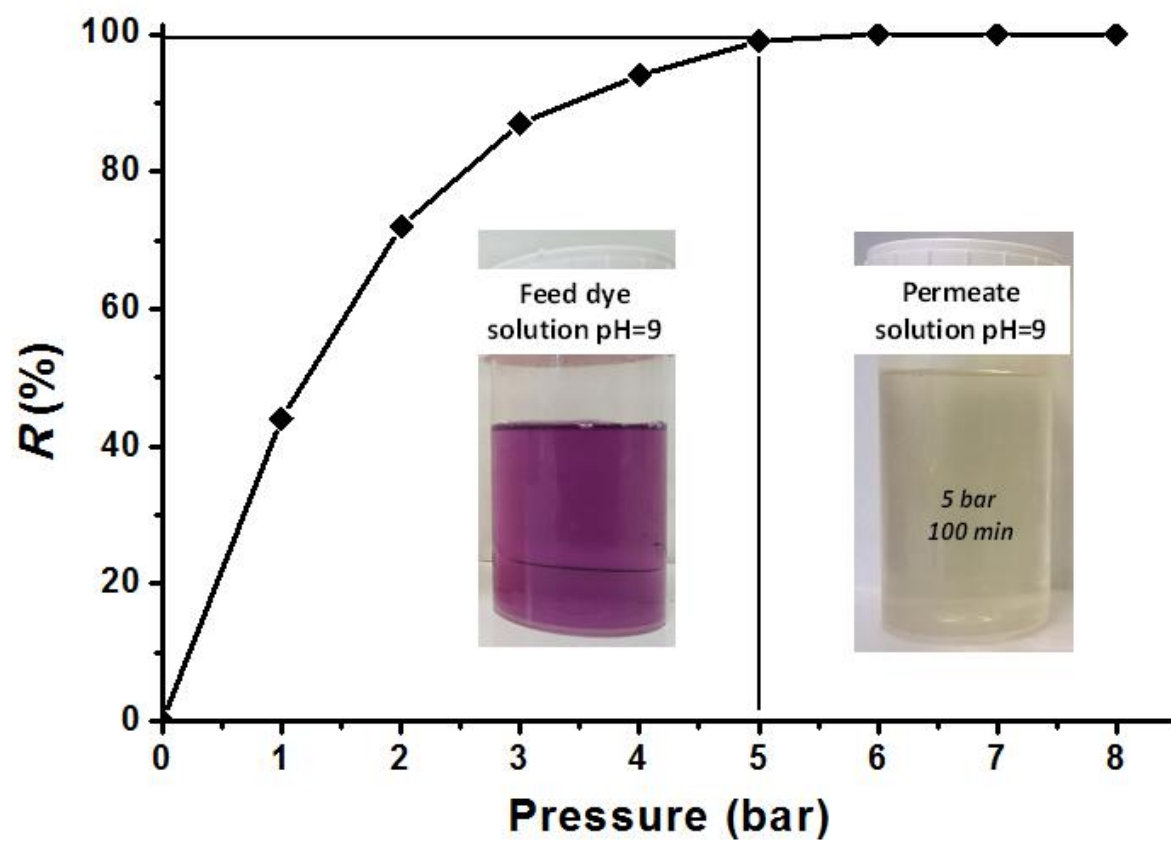


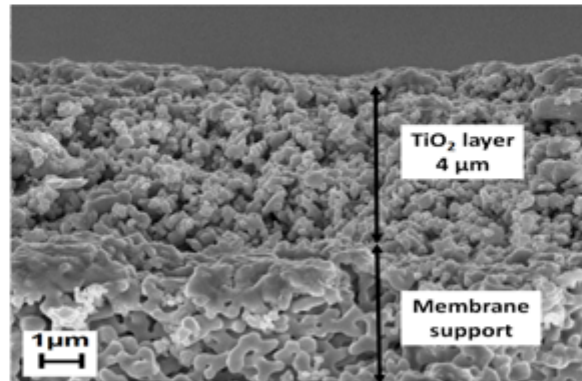
Fig. 11.



Clay/Alumina tubular support



TiO₂ membrane preparation



Ultrafiltration



**Feed dye
solution pH=9**



**Permeate
solution pH=9**



Highlights

- Preparation of low cost clay/alumina support having very good chemical and mechanical resistances.
- Formation of UFactive layer by slip casting method using a dispersion of TiO_2 nano-powders solution
- Homogeneous asymmetric UF titania membrane having 50 nm pore diameter has been obtained.
- The Titania UF membrane has a high performance towards Alizarin Red dye removal from aqueous solution.